Molecular Neurobiology (2019) 56:4086–4101
https://doi.org/10.1007/s12035-018-1352-x

AMPK Activation of PGC-1α/NRF-1-Dependent SELENOT Gene Transcription Promotes PACAP-Induced Neuroendocrine Cell Differentiation Through Tolerance to Oxidative Stress

Houssni Abid[1,2] · Dorthe Cartier[1,2] · Abdallah Hamieh[1,2] · Anne-Marie François-Bellan[3] · Christine Bucharles[1,2] · Hugo Pothion[1,2] · Destiny-Love Manecka[1,2] · Jérôme Leprince[1,2] · Sahil Adriouch[2,4] · Olivier Boyer[2,4] · Youssef Anouar[1,2] · Isabelle Lihrmann[1,2]

Received: 13 July 2018 / Accepted: 13 September 2018 / Published online: 28 September 2018

Abstract

Several cues including pituitary adenylate cyclase-activating polypeptide (PACAP), which acts through cAMP stimulation, specify the conversion of sympathoadrenal (SA) precursors toward different cell phenotypes by promoting their survival and differentiation. Selenoprotein T (SELENOT) is a PACAP-stimulated ER oxidoreductase that exerts an essential antioxidant activity and whose up-regulation is associated with SA cell differentiation. In the present study, we investigated the transcriptional cascade elicited by PACAP/cAMP to trigger SELENOT gene transcription during the conversion of PC12 cells from SA progenitor-like cells toward a neuroendocrine phenotype. Unexpectedly, we found that PACAP/cAMP recruits the canonical pathway that regulates mitochondrial function in order to elicit SELENOT gene transcription and the consequent antioxidant response during PC12 cell differentiation. This cascade involves LKB1-mediated AMPK activation in order to stimulate SELENOT gene transcription through the PGC1-α/NRF-1 complex, thus allowing SELENOT to promote PACAP-stimulated neuroendocrine cell survival and differentiation. Our data reveal that a PACAP and cAMP-activated AMPK-PGC-1α/NRF-1 cascade is critical for the coupling of oxidative stress tolerance, via SELENOT gene expression, and mitochondrial biogenesis in order to achieve PC12 cell differentiation. The data further highlight the essential role of SELENOT in cell metabolism during differentiation.

Keywords cAMP · PGC-1α · NRF-1 · Mitochondriogenesis · Oxidative stress

Introduction

Studies of sympathetic ontogeny have shown that sympathoadrenal (SA) precursors derive from the neural crest and give rise to the two catecholaminergic derivates, i.e., sympathetic neurons and chromaffin cells [1–3]. Ganglionic sympathetic neurons innervate various organs to control their vital activity, while chromaffin cells are a specialized group of neurons located principally in the adrenal medulla, which are endowed with both neuronal and endocrine features and which release catecholamines in the circulation in stress condition. Pituitary adenylate cyclase-activating polypeptide (PACAP), acting through cAMP signaling, plays an important role in this lineage. It is present and active in pre- and post-ganglionic sympathetic neuroblasts and neurons in the embryo and the adult, respectively, and is a major regulator of sympathetic/chromaffin cell activity [4–8]. Like nerve growth factor (NGF), which is instrumental to sympathetic neuron survival

Houssni Abid, Dorthe Cartier, Youssef Anouar, and Isabelle Lihrmann equally contributed to this work.

Electronic supplementary material The online version of this article (https://doi.org/10.1007/s12035-018-1352-x) contains supplementary material, which is available to authorized users.

✉ Isabelle Lihrmann
isabelle.lihrmann@univ-rouen.fr

[1] UNIROUEN, Inserm U1239, Neuronal and Neuroendocrine Differentiation and Communication Laboratory, Rouen-Normandie University, 76821 Mont-Saint-Aignan, France

[2] Institute for Research and Innovation in Biomedicine, 76000 Rouen, France

[3] CNRS UMR 7051, Neurophysiopathol Inst, Aix-Marseille University, 13015 Marseille, France

[4] UNIROUEN, Inserm U1234, Pathophysiology and Biotherapy of Inflammatory and Autoimmune Diseases, Rouen-Normandie University, 76000 Rouen, France

and differentiation, PACAP causes morphological and functional alterations in differentiating PC12 cells [9], a cell line with SA properties initially obtained from a rat adrenal tumor [10] and characterized by electrical excitability, a hallmark of both neuronal and neuroendocrine differentiation [6]. At variance with NGF, PACAP strongly regulates in these cells the expression of the neuroendocrine proteins chromogranins, which are constituents of dense-core secretory granules associated with the capacity to store and release catecholamines [6, 11, 12]. This observation indicates that the PACAP effect confers neuroendocrine properties in the SA lineage. In addition, PACAP but not NGF also up-regulated selenoprotein T (SELENOT) expression, a key oxidoreductase present in the endoplasmic reticulum (ER) [13–15] which is essential at early stages of mouse development [15, 16]. SELENOT is highly expressed in the developing nervous system, and has been shown to exert a potent protective and antioxidant effect in neurons [16–18]. For instance, targeted inactivation of SELENOT in mouse neural precursors led to a reduction of several brain structures during the first postnatal week, which results in a hyperactive behavior at adulthood [16]. A loss of immature neurons is observed in these mice, which is associated with an increase in oxidative stress [16]. In a mouse model of Parkinson's disease, SELENOT depletion in neural precursors resulted in an exacerbated increase in reactive oxygen species (ROS) and neurodegeneration in the nigrostriatal system [15, 16]. In addition to these neuroprotective effects, SELENOT also protects neuroendocrine and endocrine cells from ER and oxidative stresses, and its absence provoked Ca^{2+} store depletion, N-glycosylation defects, misfolded protein accumulation, unfolded protein response activation, and hormone production and secretion defects [13, 14, 18, 19]. Altogether, these observations suggest that stimulated SELENOT gene expression is essential to help neuronal and neuroendocrine cells to cope with ER and oxidative stress in response to high metabolic rate during differentiation and increased functional activity. To decipher the mechanisms underlying SELENOT gene induction, we first identified cis- and trans-acting elements transcriptionally regulating SELENOT expression during PACAP-promoted PC12 cell neuroendocrine differentiation. We found that SELENOT gene expression is governed by a transcriptional network that has been previously associated with mitochondrial function and ROS scavenging [20]. This signaling pathway requires the activation of the adenosine monophosphate (AMP)-dependent kinase (AMPK) and the recruitment of the peroxisome proliferator-activated receptor gamma coactivator 1-alpha (PGC-1α)/nuclear respiratory factor 1 (NRF-1) transcriptional complex to the SELENOT gene promoter. This core signaling mechanism, which controls mitochondrial function and ATP production, would concomitantly allow PC12 cells to maintain redox homeostasis which is essential for their neuroendocrine differentiation upon PACAP stimulation.

Results

SELENOT Is Essential to Cope with Oxidative Stress During Neuroendocrine Cell Differentiation

SELENOT is part of an antioxidant program induced by PACAP during neuroendocrine cell differentiation [13, 18, 21–24]. This ER-resident protein contributes to maintain ER and redox homeostasis thanks to its antioxidant activity conferred by the evolutionary conserved CXXSec sequence, Sec being a selenocystein residue, within a thioredoxin-fold [15, 16]. In line with these previous results, PC12 cells in which SELENOT levels were permanently depleted with a SELENOT shRNA lentiviral vector (65% inhibition, Fig. 1a, b) have increased ROS levels (45% increase; Fig. 1c), as compared to cells expressing a non-specific shRNA. This effect could be specifically rescued, as described before [14], by transiently expressing in the stable SELENOT shRNA-KD (knocked down) PC12 cell line a shRNA-resistant form of SELENOT mRNA including the SECIS sequence necessary for Sec incorporation (Fig. 1d). SELENOT-depleted cells also showed decreased cell viability (47% decrease; Fig. 1e), and this effect was also rescued with the shRNA-resistant form of SELENOT mRNA (Fig. 1f). Strikingly, SELENOT shRNA treatment obliterated PC12 cell differentiation, as evidenced by the impairment of PACAP (100 nM)-induced neuritic processes (Fig. 1g, h). Together, these data show that SELENOT is necessary to maintain redox homeostasis, and that its repression affects PC12 cell survival and differentiation.

The SELENOT Gene Is a NRF-1 Target

In order to understand the mechanisms underlying SELENOT gene transcription during neuroendocrine cell differentiation, PC12 cells were exposed not only to PACAP (100 nM), but also to H_2O_2 (100 μM) used to trigger oxidative stress. Both stimuli generated a quite similar time-response curve for SELENOT gene expression (Fig. 2a, b), suggesting that SELENOT gene transcription is stimulated by PACAP to protect differentiating cells against oxidative stress. Using a comparative genomic approach (multipipmaker.bx.psu.Vedu/pipmaker), we visualized several regions of conservation within the SELENOT gene 5′-flank sequence (10 kb) cleared from interspread repeats and low complexity sequences (http://www.repeatmasker.org/): one in the proximal promoter region and the other around 3500 bp. However, only the former had undergone evolutionary pressure to be conserved between mouse, rat, human, and cow (Fig. 2c; Supplemental Fig. 1), suggesting its importance for SELENOT gene regulation. This region was used to construct three promoter-deletion mutants in order to assess their transcriptional activity in PC12 cells, using a luciferase reporter assay. The constructs encompassing 306 and 159 bp exhibited a significant

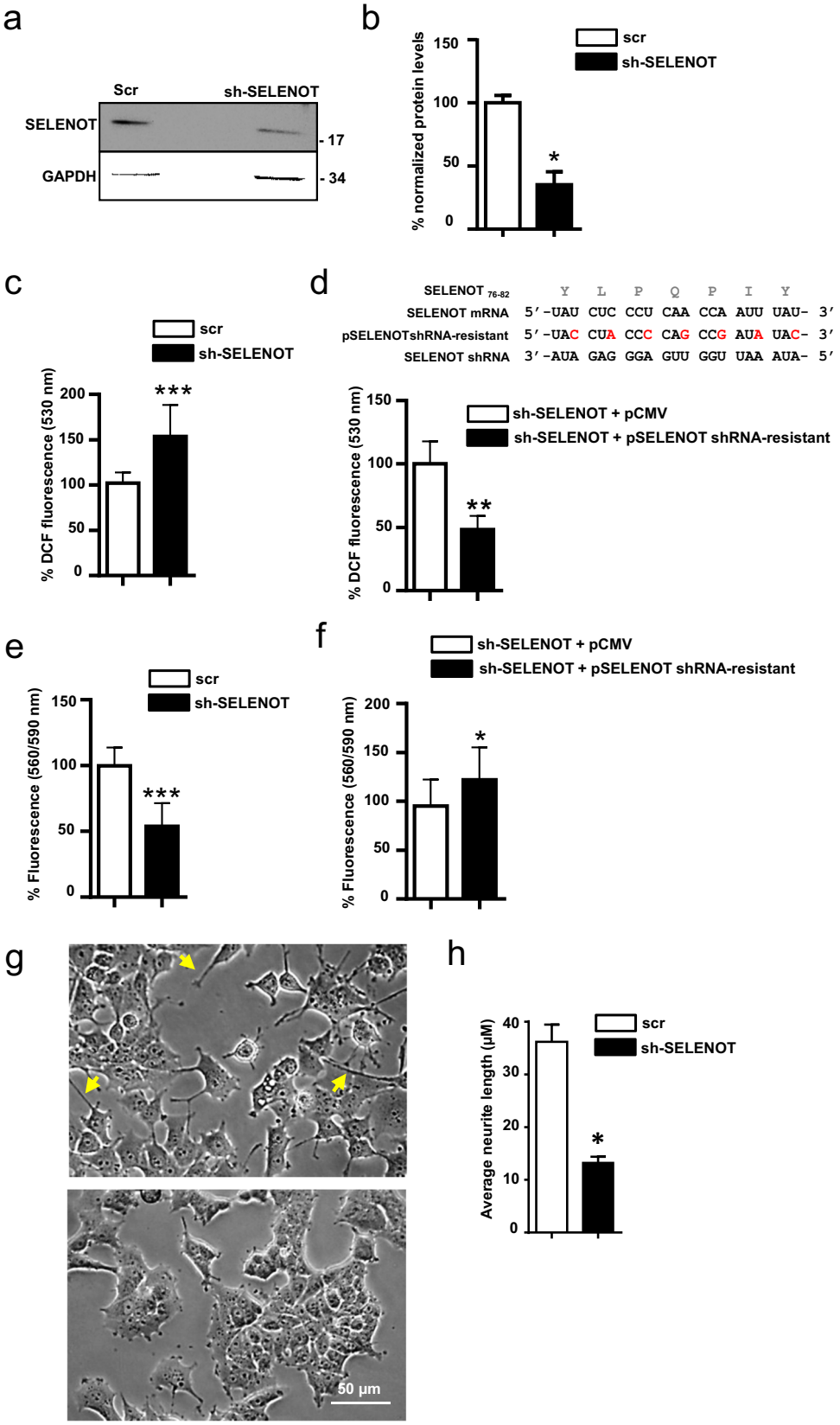
a
Scr
sh-SELENOT
SELENOT
GAPDH
- 17
- 34
b
scr
sh-SELENOT
% normalized protein levels
150
100
50
0
*
c
scr
sh-SELENOT
% DCF fluorescence (530 nm)
200
150
100
50
0
***
d
SELENOT 76-82 Y L P Q P I Y
SELENOT mRNA 5′-UAU CUC CCU CAA CCA AUU UAU- 3′
pSELENOTshRNA-resistant 5′-UAC CUA CCC CAG CCG AUA UAC- 3′
SELENOT shRNA 3′-AUA GAG GGA GUU GGU UAA AUA- 5′
% DCF fluorescence (530 nm)
sh-SELENOT + pCMV
sh-SELENOT + pSELENOT shRNA-resistant
**
e
scr
sh-SELENOT
% Fluorescence (560/590 nm)
***
f
sh-SELENOT + pCMV
sh-SELENOT + pSELENOT shRNA-resistant
% Fluorescence (560/590 nm)
*
g
50 µm
h
scr
sh-SELENOT
Average neurite length (µM)
40
30
20
10
0
*

◀ **Fig. 1** The SELENOT antioxidant response is essential for PC12 cell survival and differentiation into neuron-like cells. **a**, **b** Western blot analysis of SELENOT expression in SELENOT shRNA- and control scrambled shRNA-transduced PC12 cells. GAPDH was used as a loading control. Data are presented as mean ± SEM relative to control ($n = 4$) (*P value < 0.05; Mann-Whitney U test). **c** Transduced PC12 cells expressing SELENOT shRNA or a scrambled shRNA were incubated with the DCFDA probe for 45 min, and the fluorescence of ROS-oxidized DCF probe was measured. Data are presented as mean ± SEM relative to control ($n = 8$) (***P value < 0.001; Mann-Whitney U test). **d** Analysis of ROS levels in cells expressing the SELENOT shRNA in the absence or presence (rescued) of a recombinant shRNA-resistant form of rat SELENOT mRNA containing the SECIS sequence necessary to direct incorporation of a selenocysteine residue. The empty pCMV vector was used to assess the specificity of the rescue experiment. Data are presented as mean ± SEM relative to control ($n = 6$) (**P value < 0.01; Mann-Whitney U test). **e** PC12 cell viability was assessed after transduction with SELENOT shRNA or scrambled shRNA. Data are presented as mean ± SEM relative to control ($n = 8$) (***P value < 0.001; Mann-Whitney U test. **f** Analysis of the viability of cells expressing the SELENOT shRNA in the absence or presence (rescued) of a recombinant shRNA-resistant form of rat SELENOT mRNA containing the SECIS sequence necessary to direct incorporation of a selenocysteine residue. The empty pCMV vector was used to assess the specificity of the rescue experiment. Data are presented as mean (SD) ($n = 7$) (*P value < 0.05; Wilcoxon test). **g** Transduced PC12 cells expressing SELENOT shRNA or a scrambled shRNA were incubated with PACAP for 48 h and the number of neurites was determined using an inverted Microscope Nikon Eclipse TS100 and ImageJ software. Neurites are indicated with arrows. Data are expressed as mean ± SEM relative to control ($n = 4$ slides) (*P value < 0.05; Mann-Whitney U test)

transcriptional activity in PC12 cells (Fig. 2d), but not in Cos7 cells (data not shown), in comparison to the promoterless pGL3-basic vector. Compared to the − 159-bp construction, which presents high luciferase activity, the shorter − 64-bp construct was inactive in PC12 cells, thus indicating that important regulatory regions involved in SELENOT gene expression are included in a short promoter region comprised between positions − 159 and − 64 bp in the − 159-bp construct (Fig. 2d). Treatment of transfected PC12 cells by 100 nM PACAP for 6 h elicited a significant increase in the activity of the 306- and 159-bp promoter-containing constructs (1.57- and 1.65-fold increase, respectively) (Fig. 2d), but not of the 64-bp construct or the promoterless pGL3-basic plasmid. In agreement with the effect of PACAP through accumulation of cAMP, treatment with the adenylate cyclase activator forskolin (50 μM) for 6 h also stimulated the transcriptional activity of the constructs bearing the 306- and 159-bp cis-acting fragments (not shown). To identify putative protein binding sites in the proximal region of the SELENOT gene, we analyzed in silico the DNA sequence comprised between − 159 and − 64 bp using the MatInspector program (http://www.genomatix.de/). Exploring the degree of evolutionary conservation of putative transcription factor binding sites in the SELENOT gene promoter from different species revealed that only cis-elements known as NRF-1 binding sites, denoted NRF-1 A, B, and C, were conserved between species (Fig. 2e). NRF-1 is a basic region-leucine zipper (bZIP) transcription factor that activates the expression of nuclear genes essential for mitochondrial biogenesis and function, and some key metabolic genes regulating cellular growth [25, 26]. A mutation introduced in each of the three NRF-1 sites (Fig. 2f, upper panel) reduced the reporter activity in basal condition by at least 50% (Fig. 2f, lower panel), and abolished the PACAP (100 nM)- and forskolin (50 μM)-induced SELENOT gene-promoter transcriptional activity. Noteworthy, NRF-1-C binding site showing the highest interspecies conservation (Fig. 2e) is also the most important for SELENOT promoter activity, which is reduced by 85–90% upon NRF-1-C mutation (Fig. 2f, g). Its mutation also abolished H_2O_2 (100 μM)-induced SELENOT promoter-driven luciferase activity (Fig. 2g), further confirming the similarity of the mechanisms triggered by PACAP stimulation and oxidative stress to regulate SELENOT gene transcription. To determine whether NRF-1 associates with and regulates the SELENOT gene promoter in living PC12 cells, chromatin immunoprecipitation (ChIP) analysis was carried out. As shown in Fig. 2h, an antibody directed against NRF-1 precipitated SELENOT gene promoter fragments from PC12 cells with a 191-fold enrichment factor compared to a non-specific control antibody ($F_{1.4} = 3251$). An enrichment of comparable magnitude (174-fold enrichment compared to the non-specific control antibody, $F_{1.4} = 160.5$) was found when the rabbit polyclonal antibody against NRF-1 was used to precipitate known NRF-1 target gene promoters, namely calmodulin 3 (Calm3) promoter (Fig. 2h) and ornithine decarboxylase 1 promoter (data not shown) [27]. By contrast, the same antibody did not precipitate the non-target glyceraldehyde 3-phosphate dehydrogenase (Gapdh) gene promoter ($F_{1.4} = 6.821$). When PC12 cells were treated with PACAP (100 nM, 6 h), a greater enrichment in SELENOT promoter fragments was obtained after DNA precipitation with the anti-NRF-1 antibody ($F_{1.4} = 57.46$; Fig. 2i). This was the case neither for Calm3 ($F_{1.4} = 1.417$; Fig. 2i) nor for GAPDH promoters ($F_{1.4} = 0.313$, data not shown). In accordance, the ratio of nuclear to cytosolic NRF-1 was 1.61 ± 0.196 in basal condition, and 3.23 ± 0.242 in PC12 cells treated with PACAP, thus showing that PACAP induces a 2-fold increase in NRF-1 nuclear translocation (Fig. 2j). These results indicate that NRF-1 binds to the SELENOT gene promoter in living PC12 cells, that PACAP treatment enhances the amount of NRF-1 bound to this promoter, and that NRF-1 is indispensable to increase SELENOT gene transcription in response to PACAP, forskolin, and oxidative stress signaling

PGC-1α Binds to NRF-1 to Co-activate SELENOT Gene Transcription

PGC-1α is a transcriptional coactivator that plays a major integrative function in orchestrating a genetic program of mitochondrial biogenesis via a NRF-1-dependent pathway [26, 28,

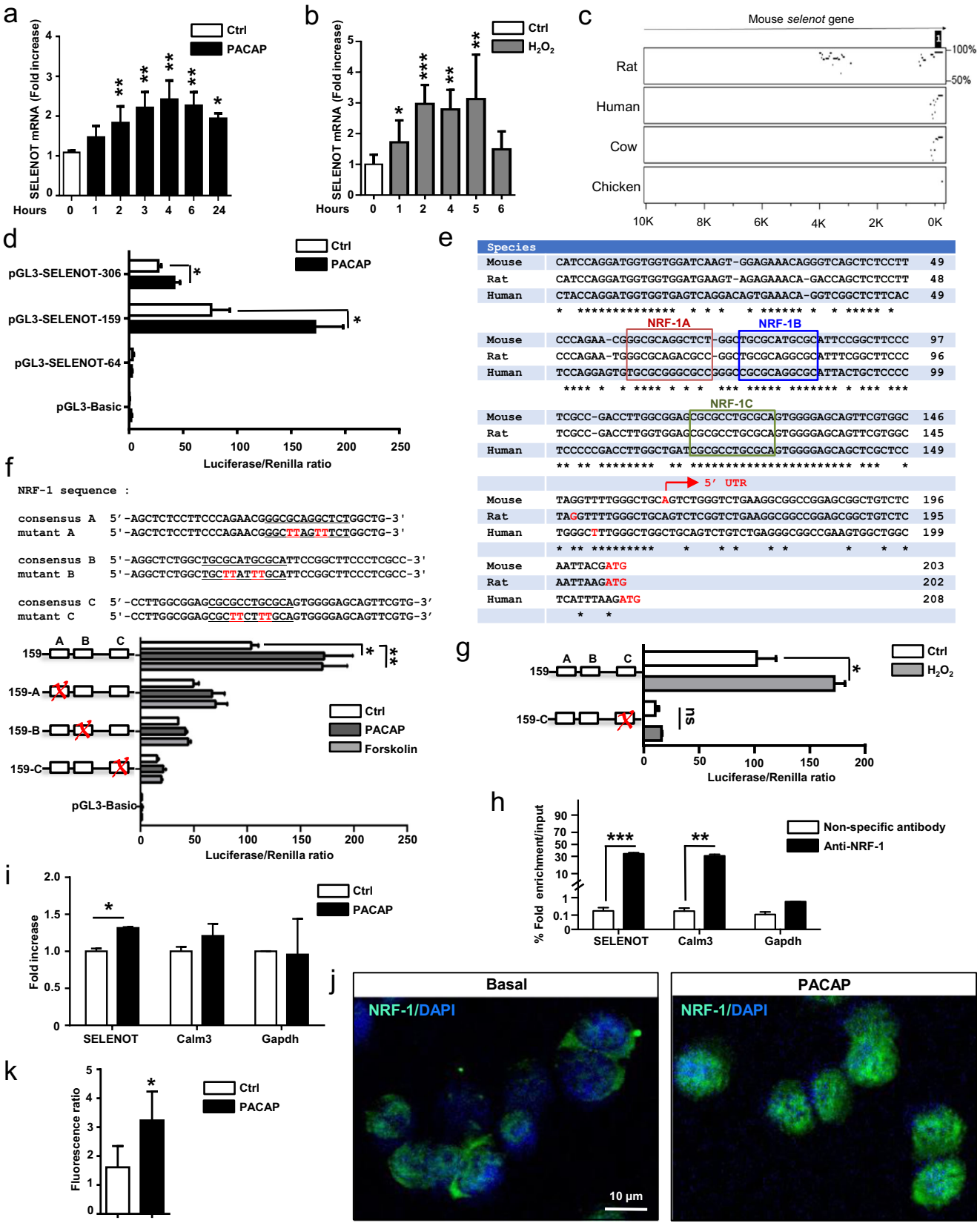
a
SELENOT mRNA (Fold increase)
Ctrl
PACAP
Hours 0 1 2 3 4 6 24
b
SELENOT mRNA (Fold increase)
Ctrl
H2O2
Hours 0 1 2 4 5 6
c
Mouse selenot gene
Rat
Human
Cow
Chicken
100%
50%
10K 8K 6K 4K 2K 0K
d
Ctrl
PACAP
pGL3-SELENOT-306
pGL3-SELENOT-159
pGL3-SELENOT-64
pGL3-Basic
Luciferase/Renilla ratio
e
Species
Mouse CATCCAGGATGGTGGTGGATCAAGT-GGAGAAACAGGGTCAGCTCTCCTT 49
Rat CATCCAGGATGGTGGTGGATGAAGT-AGAGAAACA-GACCAGCTCTCCTT 48
Human CTACCAGGATGGTGGTGAGTCAGGACAGTGAAACA-GGTCGGCTCTTCAC 49
NRF-1A
NRF-1B
Mouse CCCAGAA-CGGGCGCAGGCTCT-GGCTGCGCATGCGCATTCCGGCTTCCC 97
Rat CCCAGAA-TGGGCGCAGACGCC-GGCTGCGCAGGCGCATTTCGGCTTCCC 96
Human TCCAGGAGTGTGCGCGGGCGCCGGGCCGCGCAGGCGCATTACTGCTCCCC 99
NRF-1C
Mouse TCGCC-GACCTTGGCGGAGCGCGCCTGCGCAGTGGGGAGCAGTTCGTGGC 146
Rat TCGCC-GACCTTGGTGGAGCGCGCCTGCGCAGTGGGGAGCAGTTCGTGGC 145
Human TCCCCCGACCTTGGCTGATCGCGCCTGCGCAGTGGGGAGCAGCTCGCTCC 149
5′ UTR
Mouse TAGGTTTTGGGCTGCAGTCTGGGTCTGAAGGCGGCCGGAGCGGCTGTCTC 196
Rat TAGGTTTTGGGCTGCAGTCTCGGTCTGAAGGCGGCCGGAGCGGCTGTCTC 195
Human TGGGCTTTGGGCTGGCTGCAGTCTGTCTGAGGGCGGCCGAAGTGGCTGGC 199
Mouse AATTACGATG 203
Rat AATTAAGATG 202
Human TCATTTAAGATG 208
f
NRF-1 sequence :
consensus A 5′-AGCTCTCCTTCCCAGAACGGGCGCAGGCTCTGGCTG-3'
mutant A 5'-AGCTCTCCTTCCCAGAACGGGCTTAGTTTCTGGCTG-3'
consensus B 5'-AGGCTCTGGCTGCGCATGCGCATTCCGGCTTCCCTCGCC-3'
mutant B 5'-AGGCTCTGGCTGCTTATTGCATTCCGGCTTCCCTCGCC-3'
consensus C 5′-CCTTGGCGGAGCGCGCCTGCGCAGTGGGGAGCAGTTCGTG-3′
mutant C 5'-CCTTGGCGGAGCGCTTCTTTGCAGTGGGGAGCAGTTCGTG-3′
A B C
159
159-A
159-B
159-C
pGL3-Basic
Ctrl
PACAP
Forskolin
Luciferase/Renilla ratio
g
A B C
159
159-C
ns
Ctrl
H2O2
Luciferase/Renilla ratio
h
% Fold enrichment/input
Non-specific antibody
Anti-NRF-1
SELENOT
Calm3
Gapdh
i
Fold increase
Ctrl
PACAP
SELENOT
Calm3
Gapdh
j
Basal
PACAP
NRF-1/DAPI
10 μm
k
Fluorescence ratio
Ctrl
PACAP

Fig. 2 The SELENOT gene is a NRF-1 target. **a**, **b** Time-dependent effect of PACAP (100 nM) (**a**) and H_2O_2 (100 μM) (**b**) on SELENOT mRNA levels. Data are presented as mean ± SEM relative to control ($n = 3$–6) (*P value < 0.05; **P value < 0.01, ***P value < 0.001; Mann-Whitney U test). **c** MultiPipMaker analysis of sequences flanking the SELENOT gene in different species. In this diagram, the 5′-region (from 0 to 10,000 bp) flanking mouse SELENOT gene was compared with orthologous sequences obtained from different mammalian and non-mammalian species. Percent identity (50–100%) is shown on y-axis. Distance from the transcription start site (0 K) is shown below the sequence identity plots. Exon 1 is marked above the sequence identity plot with a black box. MultiPipMaker was performed at http://pipmaker.bx.psu.edu/cgi-bin/multipipmaker. Mouse: (gb|AC119873.38|); rat: (Ensembl Rnor_5.0 (GCA_000001895.3), human: (gb|AC069236.27|); cow: (Ensembl UMD 3.1); chicken: (Ensembl Galgal4). **d** Sequential deletion constructs of the 306-bp SELENOT promoter were generated and tested for their ability to drive luciferase activity from the pGL3-Basic vector in control and PACAP (100 nM)-treated cells for 6 h. Results are presented as firefly luciferase/renilla luciferase ratio. Each value is the mean ± SEM ($n = 3$–10) (*P value < 0.05, Mann-Whitney U test). **e** In silico alignment of the 5′-proximal regions of the mouse, rat, and human SELENOT promoters. Putative NRF-1 binding sites termed NRF-1 A–C are indicated by open squares (the green box in NRF-1C displayed the highest bioinformatic score). Interspecies nucleotide conservation is indicated by asterisks. The putative transcription start in the 5′-UTR is marked by the arrow. **f** Three constructs with mutations in the NRF-1 consensus binding sites of the pGL3-SELENOT-159 bp vector were generated and tested for their ability to drive luciferase activity. PACAP (100 nM) and forskolin (50 μM) effects were assessed after a 6-h treatment of PC12 cells. The sequences of the consensus and mutant NRF-1 oligonucleotides are indicated in the upper panel. The core NRF-1 binding site is underlined, and inactivating mutations in the core consensus are depicted in bold. In the lower panel, point mutations of the identified NRF-1 sites (black boxes) are indicated by X. Each value is the mean ± SEM ($n = 4$–8) (*P value < 0.05; **P value < 0.01, Mann-Whitney U test). **g** The construct with a mutation in the NRF-1-C consensus binding site in the pGL3-SELENOT-159 bp vector was tested for its ability to drive luciferase activity after a treatment with 100 μM H_20_2. Each value is the mean ± SEM ($n = 4$) (*P value < 0.05, Mann-Whitney U test). **h**, **i** ChIP analysis of the interaction of endogenous NRF-1 with the rat SELENOT promoter in control conditions or in the presence of PACAP 100 nM for 6 h. Calm3 and Gapdh promoters were used as positive and negative controls, respectively. Data are presented as mean ± SEM relative to control ($n = 3$) (*P value < 0.05; **P value < 0.01; ***P value < 0.001, two-way ANOVA). **j**, **k** Immunocytochemical analysis showing the nuclear translocation of NRF-1 in PC12 cells incubated with PACAP (100 nM) for 2 h. The ratio of fluorescence intensity in the nuclei to that in the cytoplasm were calculated from confocal Z stack images shown in Fig. 2j, by drawing regions of interest around several nuclei and the cytoplasm using PhotoFilter Studio X and ImageJ. Data are presented as mean ± SEM relative to control ($n = 14$–17) (***P value < 0.001, Mann-Whitney U test)

29]. Since it is a powerful regulator of ROS metabolism as well [26, 30], we examined the possibility that the PGC-1α is required for SELENOT gene expression. We found that PACAP increases PGC-1α gene expression after 2 h of treatment, with a maximal effect (6.2-fold) observed at 4 h and a decrease to nearly basal level after 6 h of treatment (Fig. 3a). PGC-1α protein levels were maximally increased at 6 h (2.97-fold) of treatment with PACAP (Fig. 3b, c). A siRNA targeting PGC-1α (Fig. 3d) strongly reduced (73%) the PACAP-induced SELENOT gene expression (Fig. 3e). In addition, immunoprecipitation experiments using NRF-1 antibodies revealed that PGC-1α and NRF-1 do interact in both undifferentiated and PACAP-differentiated PC12 cells (Fig. 3f). Further supporting a functional NRF-1/PGC-1α interaction, we showed that forskolin (50 μM), used to mimic the PACAP effect, induces well-known PGC-1α/NRF-1 target genes such as Tfam, which controls mitochondrial DNA replication and transcription, and CytC, encoding an essential component of the electron transport chain [28, 31] (Fig. 3g). Concurrently, PACAP increased by ~30% mitochondrial DNA and biomass (Fig. 3h, i). Taken together, these data indicate that SELENOT gene transcription is PGC-1α-dependent, and that increased levels of PGC-1α/NRF-1 complexes concomitantly stimulate mitochondrial biogenesis and SELENOT gene transcription.

AMPK Activation Promotes SELENOT Gene Expression and PC12 Cell Differentiation

We next sought to elucidate the mechanisms by which PACAP stimulates SELENOT gene expression upstream of PGC-1α during PC12 cell differentiation. Two kinases, p38MAPK and AMP-activated protein kinase (AMPK), are known to control PGC-1α phosphorylation [32, 33]. Inhibition of p38 MAPK using SB203580 (10 μM) did not alter PACAP-induced SELENOT gene expression, while a specific AMPK inhibitor, Compound C (CC, 5 μM), reduced by ~60% the PACAP effect (Fig. 4a). Since SELENOT gene expression is linked to a high metabolic rate in endocrine cells [14], we focused on AMPK, a key metabolic rheostat activated in response to a low cellular energy charge [34–36], which adjusts NRF-1 binding activity, cytochrome c content, and mitochondrial density [37]. siRNA-mediated knockdown of AMPKα provoked a 40% reduction in both protein (Fig. 4b) and mRNA (Fig. 4c) levels, leading to a 40% reduction in PACAP-induced SELENOT mRNA levels (Fig. 4d). Also, incubation with PACAP for different times (5–60 min) stimulated the phosphorylation of Thr172 within AMPKα (1.55-fold after 15 min), while total AMPKα protein levels were unchanged (Fig. 4e, f). In addition, AMPK activation was able to trigger SELENOT expression since treatment of PC12 cells with 0.5 mM 5-aminoimidazole-4-carboxamide 1-β-D-ribofuranoside (AICAR), an analog of AMP, increased in a time-dependent manner SELENOT protein levels up to 30% (Fig. 4g, h). AICAR also elicited an increase in PGC-1α protein levels, with a maximum (2-fold) at 24 h (Fig. 4g, h). Like PACAP, AICAR was able to trigger the differentiation of PC12 cells which showed prominent neuritic extensions after a 24-h treatment (Fig. 4i, j). We further dissected the upstream cascade leading to PACAP-stimulated AMPK phosphorylation. AMPK can be activated by upstream AMPK kinases (AMPKK) comprising calmodulin-dependent protein kinase kinase β (CAMKKβ) and liver kinase B1 (LKB1) [38]. A selective inhibitor of CAMKKβ, STO-609 (10 μM), did not alter the PACAP-stimulated SELENOT gene

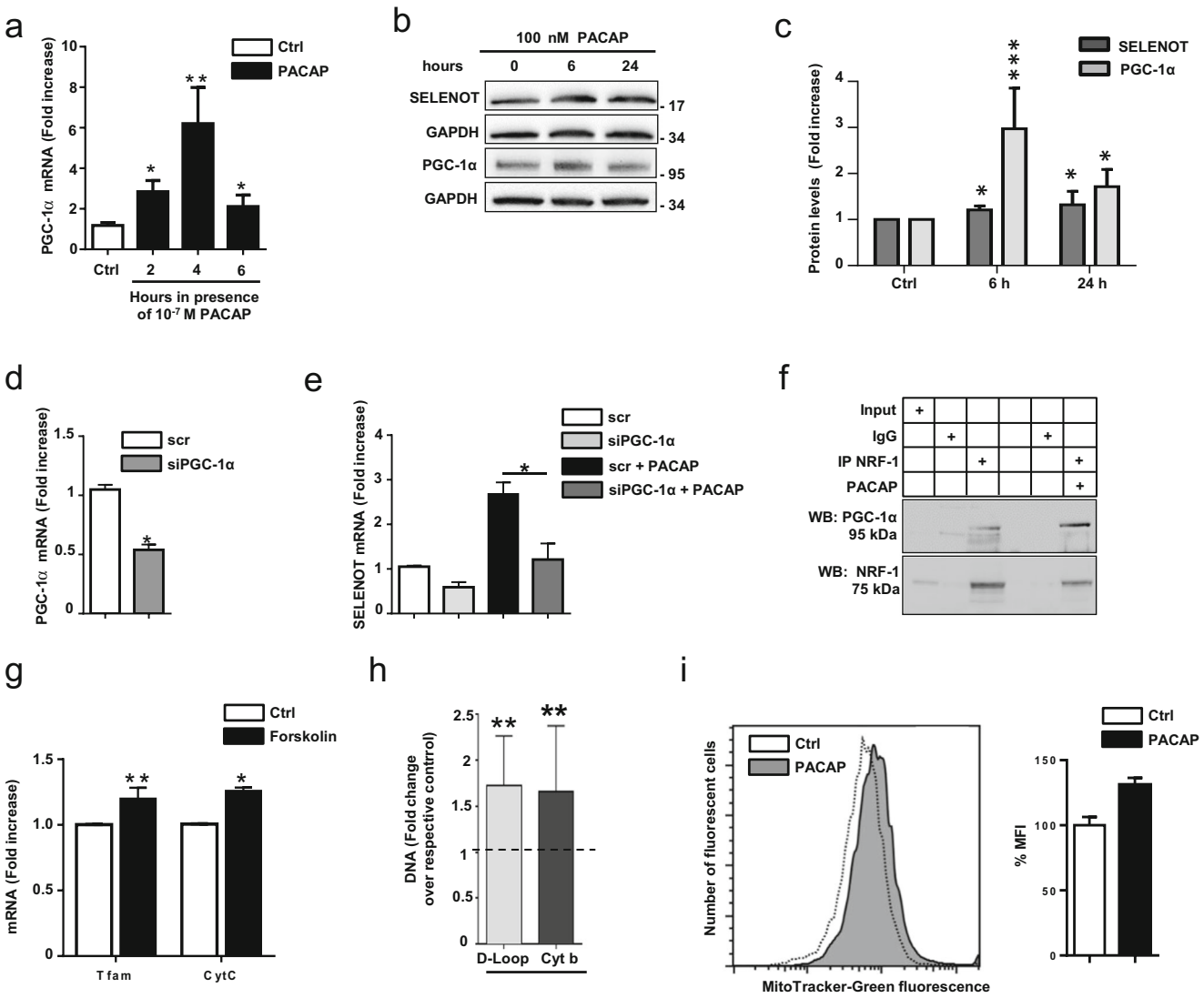

Fig. 3 PGC-1α binds to NRF-1 and is essential to co-activate SELENOT gene transcription. **a** qRT-PCR analysis showing the time-dependent effect of PACAP (100 nM) on PGC-1α mRNA levels. Data are presented as mean ± SEM relative to control ($n = 3$–5) (*P value < 0.05; **P value < 0.01, Mann-Whitney U test). **b**, **c** Western blot analysis of the time-dependent effect of PACAP (100 nM) on SELENOT and PGC-1α expression. Data are presented as mean ± SEM relative to control ($n = 5$–7) (*P value < 0.05; ***P value < 0.001, Dunn's multiple comparisons test). **d** Effect of PGC-1α knockdown on PGC-1α levels. A scrambled RNA was used as a control to assess the specificity of the interference strategy. Data are presented as mean ± SEM relative to control ($n = 4$) (*P value < 0.05, Mann-Whitney U test). **e** Effect of PGC-1α knockdown on SELENOT gene expression after a treatment with PACAP (100 nM) for 6 h. A scrambled RNA was used as a control to assess the specificity of the interference strategy. Data are presented as mean ± SEM ($n = 5$) (*P value < 0.05, Mann-Whitney U test). **f** Co-immunoprecipitation analysis of NRF-1 and PGC-1α interaction in PC12 cells in basal conditions and after a treatment with PACAP (100 nM) for 6 h. IgG, non-specific control antibody. **g** qRT-PCR analysis showing the effect of forskolin (50 μM, 6 h) on Tfam and CytC gene expression ($n = 3$–6). (*P value < 0.05, Mann-Whitney U test). **h** mtDNA copy number was assessed after a treatment with PACAP (100 nM) for 72 h as the ratio of mitochondria-encoded cytochrome b (Cyt b) and D-loop DNA copies to nucleus-encoded pyruvate kinase DNA copies via qPCR. Data are presented as mean ± SEM relative to control ($n = 5$) (**P value < 0.01, Mann-Whitney U test). **i** Analysis by flow cytometry of the fluorescence of PC12 cells stained with MTG for 30 min, treated or not with PACAP (100 nM) for 72 h, and analyzed by flow cytometry. Graph illustrating a typical response. Data are presented as mean ± SEM

expression (Fig. 4k), thus ruling out an effect of CAMKK in this cascade. In contrast, silencing LKB1 expression (80% of control, Fig. 4l, m) through siRNA treatment reduced by 40% PACAP-induced SELENOT gene expression (Fig. 4n), indicating that LKB1 participates, at least partially, in this signaling cascade.

Discussion

It has been shown that a major limitation in cell reprogramming efficiency is cell death at a check point before conversion, which could be overcome by antioxidant

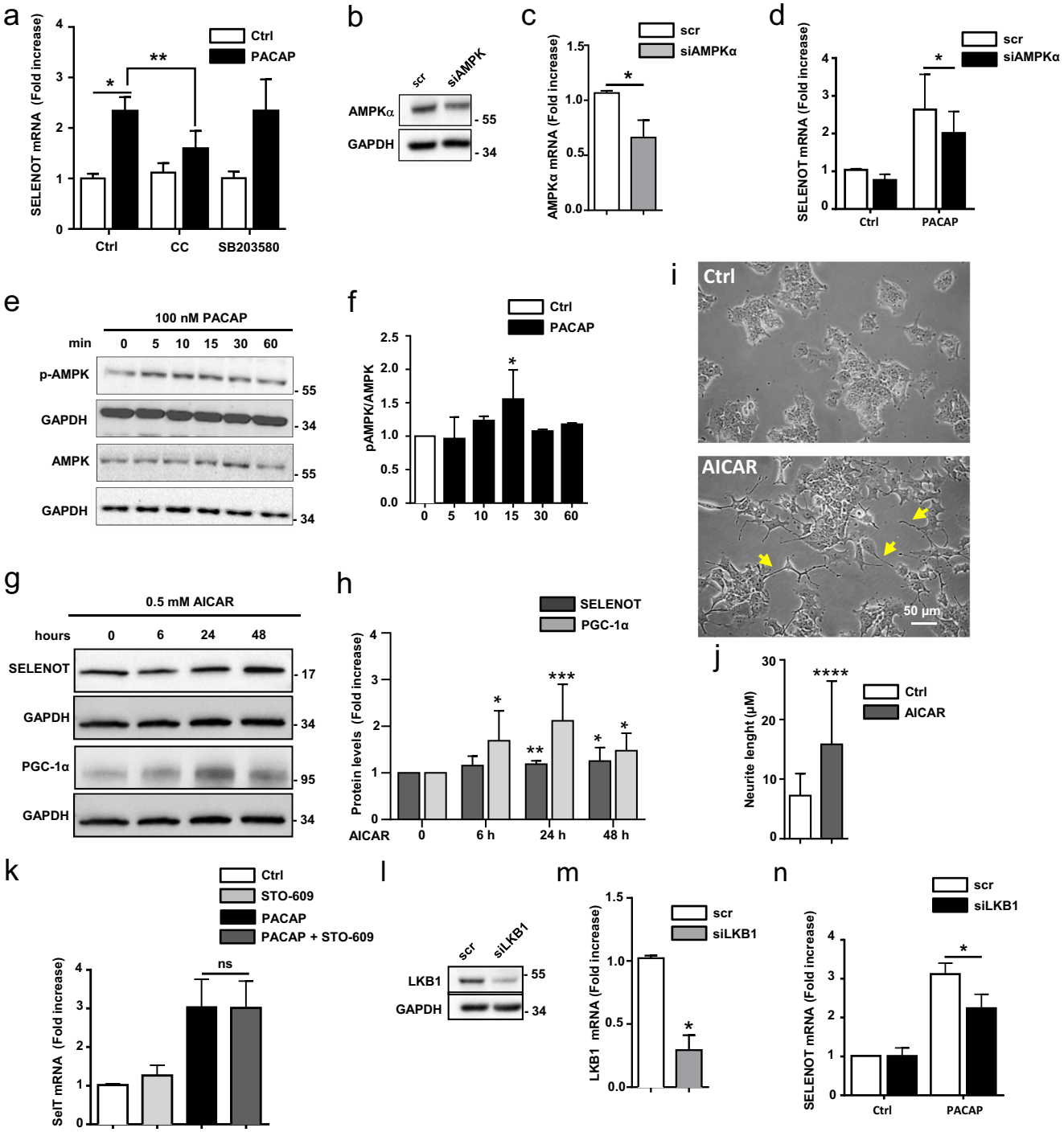

treatments [39]. Indeed, nerve cell differentiation, or transdifferentiation, requires several biological events including cell growth arrest, cell survival, neuritogenesis, and acquisition of functional characteristics, processes involving oxidative metabolism changes ineluctably resulting in high ROS production. PACAP is a potent PC12 cell neurogenic reprogramming factor [40–43], whose trophic effect is associated to its antioxidant action [13, 21–24]. Using the PACAP-regulated gene encoding SELENOT, a key antioxidant protein [15, 16], we uncovered here an unprecedentedly described transcriptional network, which converges on the transcription factor NRF-1, and couples AMPK with SELENOT antioxidant response during PC12 cell reprogramming toward a neuroendocrine phenotype. Thus, in addition to the canonical PKA signaling pathway which exerts a prosurvival role in PC12 cells [4, 5, 44, 45], we found here that PACAP-induced PC12 cell differentiation also involves AMPK activation. The AMPK-activated pathway, which is the canonical

Fig. 4 AMPK activation promotes SELENOT gene expression and PC12 cell neuronal differentiation. **a** qRT-PCR analysis showing the effect of PACAP (100 nM) on SELENOT mRNA levels in the presence of SB203580 and compound C (CC). Data are presented as mean ± SEM relative to control ($n = 4$–8) (*P value < 0.05; **P value < 0.01, Mann-Whitney U test). **b** Effect of AMPKα knockdown on AMPKα gene expression. A scrambled siRNA has been used as a control. Data are presented as mean ± SEM relative to control ($n = 4$) (*P value < 0.05, Mann-Whitney U test). **c** Effect of AMPKα knockdown on SELENOT gene expression in PC12 cells treated by PACAP (100 nM) for 6 h. A scrambled siRNA has been used as a control. Data are presented as mean ± SEM relative to control ($n = 5$) (*P value < 0.05, two-way ANOVA). **e**, **f** Comparison of the levels of AMPKα protein phosphorylated at Thr^{172} with total levels of AMPKα protein in PC12 cells treated 5–60 min with vehicle or PACAP (100 nM). Data are presented as mean ± SEM relative to control ($n = 3$–5) (*P value < 0.05, Mann-Whitney U test). **g**, **h** Western blot analysis of the time-dependent effect of AICAR (0.5 mM) on SELENOT and PGC-1α protein levels. Data are presented as mean ± SEM relative to control ($n = 3$–7) (*P value < 0.05; **P value < 0.01; ***P value < 0.001, one-way ANOVA). **i**, **j** PC12 cells were incubated with AICAR for 24 h. **i** Neurite formation was observed on an inverted Microscope Nikon Eclipse TS100. **j** Neurite length was quantified. Data are presented as mean ± SEM relative to control ($n > 30$) (****P value < 0.0001, one-way ANOVA). **k** qRT-PCR analysis of the effect of STO-609, a CAMKK inhibitor, on SELENOT gene expression. Data are presented as mean ± SEM relative to control ($n = 5$). ns; non-specific. **l**, **m** Effect of LKB1 knockdown on LKB1 protein (**l**) and mRNA (**m**) expression. A scrambled siRNA has been used as a control. Data are presented as mean ± SEM relative to control ($n = 4$) (*P value < 0.05, Mann-Whitney U test). **n** Effect of LKB1 knockdown on SELENOT gene expression in the absence or presence of PACAP 100 nM for 6 h. A scrambled siRNA has been used as a control. Data are presented as mean ± SEM relative to control ($n = 4$) (*P value < 0.05, two-way ANOVA)

signaling route to stimulate mitochondrial biogenesis, would also trigger a SELENOT-mediated antioxidant response, thus allowing PC12 cells to negotiate the metabolic changes and progress through neuroendocrine differentiation.

The intervention of AMPK in the antioxidant signaling cascade, in addition to the increase in mitochondrial biomass, supports the idea that there is a major metabolic change during PACAP-induced conversion of PC12 cells into neuroendocrine-like cells. AMPK is a key energy-sensing kinase and the guardian of energy homeostasis, which is thought to reduce protein synthesis and cell growth pathways that consume ATP, while activating carbohydrate and fatty acid oxidation to restore ATP levels [34, 46, 47]. It reprograms cellular metabolism through phosphorylation of numerous target proteins, including PGC-1α. AMPK is generally activated in response to a low cellular energy charge [35] and is also a metabolic target of GPCRs, in particular Gs-coupled receptors positively linked to adenylate cyclase, such as β adrenoreceptors in adipocytes or the heart, and melanocortin receptors in the hypothalamus [38]. We provide herein the first evidence that AMPK is also activated by the PAC1/Gs-coupled receptor during neuroendocrine cell survival and differentiation, in agreement with previous reports showing a role of AMPK in the preservation of neuronal integrity [48–52]. For example, the AMPK/NRF-1 cascade has been proposed to contribute to mitochondrial biogenesis and ischemic tolerance in neurons [53]. AMPK also limits oxidative stress and protects against the toxicity of β-amyloid peptides in Alzheimer's disease [54], as well as the toxicity of mutant huntingtin [55] and that of α-synuclein [50]. In PC12 cells, AMPK protects against stress-induced apoptosis [56]. The underlying mechanism of the AMPK neuroprotective effect is poorly documented. In skeletal muscle, it has been shown that AMPK regulates NRF-1 binding activity, cytochrome c content, and mitochondrial density during exercise training or chronic energy deprivation [37]. Our study now demonstrates that AMPK, through a PGC-1α/NRF-1 cascade, concurrently stimulates mitochondrial function and the antioxidant SELENOT during nerve cell conversion as shown using PC12 cells as a model. AMPK activation via AICAR treatment also stimulates neuritogenesis in PC12 cells, as described previously in neurons [51], indicating that the dual action of this kinase to increase cell metabolism and eliminate oxidative stress allows the successful achievement of differentiation in nerve cells.

Our study also showed that NRF-1, a bZIP transcription factor which activates the expression of nuclear genes essential for mitochondrial biogenesis and function, and some key metabolic genes regulating cellular growth [25, 57], is also involved in the control of the essential SELENOT gene. Although large scale studies have been previously performed to identify NRF-1 target genes, based on bioinformatics and ChiP-seq analysis [25, 27, 58], SELENOT was not described as a NRF-1 target gene until now. In fact, many genes encoding detoxifying, antioxidant, and glutathione-biosynthetic and metabolic enzymes are under the control of Nrf2 which binds to the ARE cis-acting sequence, thus constituting the Nrf2 regulon [59], but a role of NRF-1 in the antioxidant defense strategy has been poorly documented as yet, except for the regulation of peroxiredoxin 3 and 5 genes [60]. NRF-1 binding sites are also present in the gene encoding bcl-2 [27], which affects the reprogramming and speed of neuron conversion through an antioxidant mechanism, independently of its canonical apoptotic function [39]. Also of note, several neurodegenerative disease-related genes linked to Parkinson and Alzheimer diseases [25] are putative NRF-1 targets as evidenced by Chip-seq analysis, such as the DJ-1 gene which is known for its antioxidant function in neurons [61]. Several other observations reinforce the idea that SELENOT is a key NRF-1 target gene. For instance, SELENOT gene knockout [15] phenocopies NRF-1 gene abrogation in mice [62]. Both mutated mouse strains die at the time of embryo implantation. Mitochondrial DNA instability has been observed in NRF-1 null mice, but in comparison with Tfam-null mice, it has been proposed that mitochondrial dysfunction could not fully explain the early death of NRF-1-depleted mice [63], indicating that there are probably other vital NRF-1 targets such as SELENOT. In Drosophila and Zebrafish, disruption of NRF-1 orthologs leads to a severe neurological deficiency [64, 65]. NRF-1 null zebrafish are characterized by neuronal death and a marked brain size reduction [64], a phenotype which is reminiscent of that obtained in mice with SELENOT gene obliteration in

neuronal precursors [16, 18, 64]. Furthermore, NRF-1 activation stimulates neurite outgrowth [66], and SELENOT gene deficiency abrogates neurite outgrowth (this study). Altogether, these data show that NRF-1, in addition to its major role in mitochondrial biogenesis [25, 26, 67], is also able to trigger the antioxidant system during neural cell differentiation or reprogramming as observed here in PACAP-treated PC12 cells.

LKB1 is at least partially required for AMPK activation in PACAP-stimulated PC12 cells (this study) like in cortical neurons, although CaMKKβ is also frequently described as a major effector of AMPK in neurons [51, 68]. The functional link between the PAC1 receptor and LKB1 is not known yet. The presence of a PKA phosphorylation site at Ser^{431} of LKB1 [69] suggests that the PAC1-cAMP-PKA pathway [4, 5, 44, 70–73] might promote LKB1 activation. However, in a previous study the use of H-89, a PKA inhibitor, only partially inhibited PACAP-induced SELENOT gene expression [13], suggesting the existence of multiple signaling pathways leading to stimulation of SELENOT gene transcription in response to PACAP. In agreement, it is well established that neuritogenesis is cAMP-, Rap-1-, and ERK-dependent and requires the neuritogenic cAMP sensor Rapgef2, but is PKA-independent [4, 74], arguing again for the existence of alternative pathways activated by PACAP that remains to be fully elucidated.

Based on the data reported in the present study, we propose a model (Fig. 5) depicting the linear pathway involving LKB1, AMPK, PGC-1α, and NRF-1 by which a neurogenic factor like PACAP connects mitochondrial biogenesis and an adaptive antioxidant response involving SELENOT. Using this signaling mechanism, PC12 cells can negotiate the metabolic changes necessary to avoid their demise, and achieve a successful PACAP-induced neuroendocrine differentiation. Our data are thus in line with a recent study showing that limiting oxidative stress allows cells to cross a metabolic checkpoint and to undergo neuronal reprogramming [39].

Materials and Methods

Chemicals and Reagents

The 38-amino acid form of PACAP (PACAP-38) was obtained from Bachem (Merck Chimie, Fontenay-sous-Bois). Forskolin and STO-609 were purchased from Sigma-Aldrich (Saint Quentin Fallavier, France) and SB-203580, compound C, and AICAR from Abcam (Cambridge, UK).

Antibodies

Antibodies against phospho-AMPKα (p-AMPKα; Thr^{172}) and AMPKα were purchased from Cell Signaling Technology (Ozyme, Saint-Quentin-en-Yvelines, France). A polyclonal SELENOT antibody was obtained from Acris Antibodies GmbH (Herford, Germany), a mouse monoclonal anti-GAPDH from Invitrogen (Thermo Fisher Scientific, Villebon-sur-Yvette, France), and a mouse anti-α-Tubulin from Sigma-Aldrich. A polyclonal antibody against PGC-1α and a monoclonal NRF-1 antibody were acquired from Abcam.

Cell Culture and Treatments

PC12 cells were purchased from the European Collection of Cell Culture (ECACC, Salisbury, Wiltshire, UK) and maintained in Dulbecco's modified eagle medium (Thermo Fisher Scientific) supplemented with 10% horse serum (Invitrogen, Thermo Fisher Scientific), 5% fetal bovine serum (PAA Laboratories, Velizy-Villacoublay, France), 100 U/ml penicillin, 100 μg/ml streptomycin, and 2 mM L-glutamine (Thermo Fisher Scientific), at 37 °C in 5% CO_2 humidified atmosphere. The medium was renewed every 2–3 days. PC12 cells were plated in six-well plates and were treated with 100 nM PACAP, 50 μM forskolin, 100 μM H_2O_2, or 0.5 mM AICAR before harvesting. Inhibitors were added 1 h before and during the 24-h treatment with PACAP. siRNA transfection was carried out using the Amaxa Nucleofactor system (Lonza). RNA isolation and protein extraction were carried out 48 and 72 h later in order to quantify the knockdown efficiency by qPCR and western blotting, respectively.

Production and Transduction of Lentivirus

The lentiviral constructs containing a shRNA (5′- UAU CUC CCU CAA CCA AUU UA -3′) targeting rat SELENOT or a scrambled control shRNA (5′-GAG AAC GAG UCA CUU CACUAU-3′) were generated in the VIRHD-EP vector [75]. The constructs were sequence-verified. HEK-293T cells were co-transfected using polyethyleneimine (Polysciences, Eppelheim, Germany) with the shRNA lentiviral vector along with pCMVdR8.74 (packaging) and pMD2.G (envelope) plasmids. Two days after transfection, the conditioned media were collected, supplemented with 8 μg/ml polybrene, and added for overnight incubation to freshly plated PC12 cells for transduction. Two days after infection, the cells were selected in 1 μg/ml puromycin.

Measurement of Cell Viability and Intracellular ROS Levels

The number of viable cells was determined using the CellTiter-Blue® cell viability assay (Promega, Charbonnières les Bains, France) and the levels of intracellular ROS were measured by using DCFDA Cellular ROS Detection Assay Kit (Abcam) following the manufacturer instructions. The fluorescence of ROS-oxidized 2′,7′-dichlorofluorescin (DCF) was measured at 530 nm. For the SELENOT rescue experiment, the pCMV vector containing the rat SELENOT cDNA mutated in the SELENOT shRNA recognition sequence was electroporated

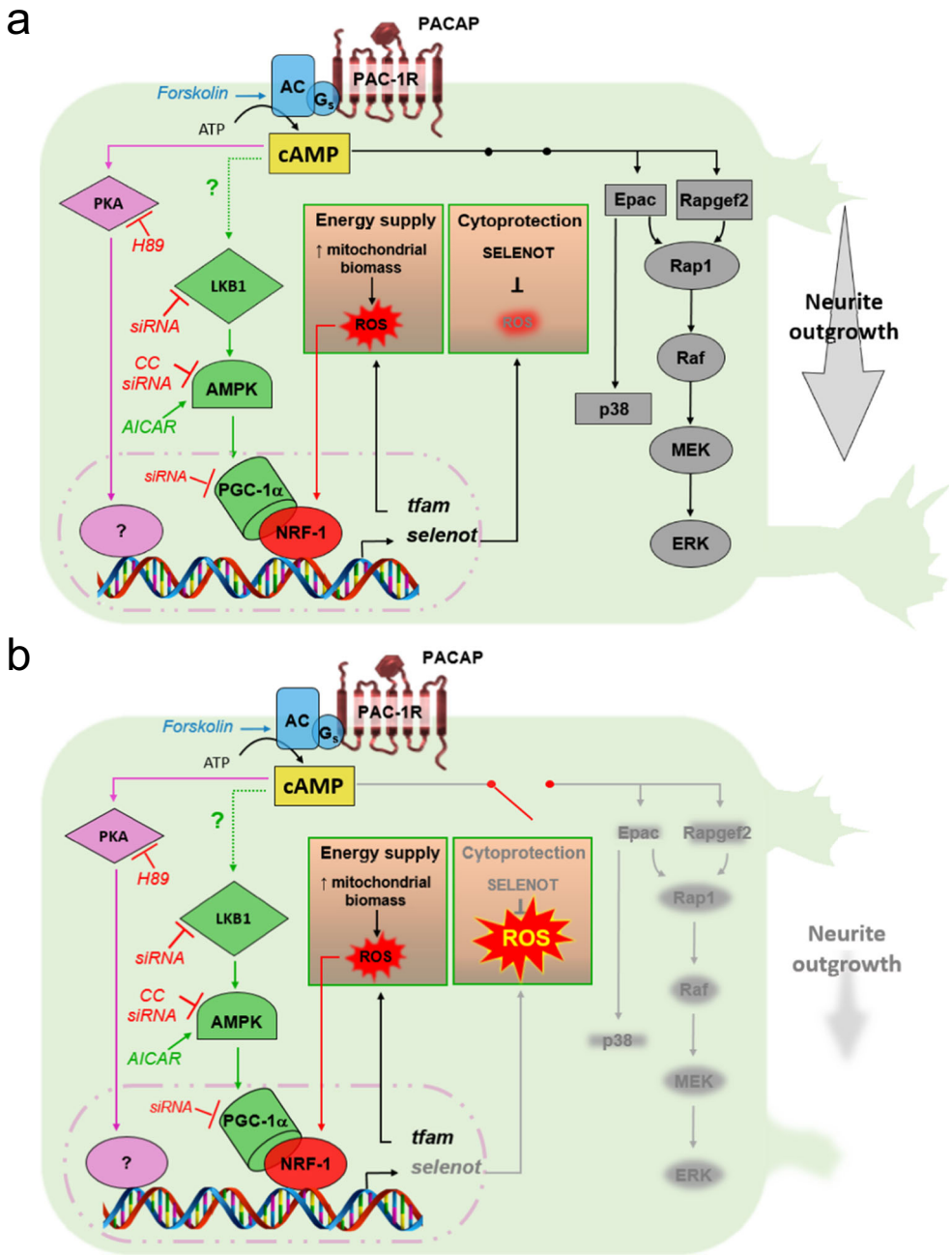

Fig. 5 Schematic representation summarizing how the LKB1/AMPK/PGC-1α/NRF-1 signaling cascade connects metabolic changes and SELENOT antioxidant response during PACAP-induced PC12 cell neuroendocrine differentiation. **a** Elevation of cAMP following PAC1 receptor activation leads to activation of at least three cAMP sensors (PKA, Epac, and Rapgef2) all involved in some aspects of PC12 cell differentiation. In addition, the neurogenic PACAP/PAC1 system triggers PC12 cell differentiation through activation of phosphorylation cascades involving LKB1, AMPK, PGC-1α, and NRF-1 as the downstream effector. On one side, PGC-1α in association with NRF-1 orchestrates the transcriptional stimulation of mitochondrial genes, ultimately leading to an increase in mitochondrial biomass, which is associated with ROS production and toxicity. On the other side, the PGC-1α/NRF-1 complex also activates the gene transcription of SELENOT which plays an important role in ROS detoxification and cytoprotection. Using this mechanism, PC12 cells can negotiate the metabolic change elicited by PACAP, avoiding death and achieving neuronal differentiation through activation of other cAMP sensors, such as Epac, and Rapgef2, both involved in neuritogenesis and other differentiation hallmarks. **b** Cytoprotection is failing in cells that lack SELENOT and ROS levels become toxic and prevent progression to other stages of differentiation

in stably SELENOT shRNA-expressing PC12 cells using the Amaxa Nucleofactor system (Lonza, Basel, Switzerland). ROS levels were measured 48 h later as described above. The empty pCMV vector was used to assess the rescue specificity.

Analysis and Cloning of the SELENOT Gene Promoter

SELENOT gene upstream sequences (up to 10 kb) from different species (human, mouse, rat, cattle, chicken) were extracted from genomic databases (http://www.ensembl.org/), and interspersed repeats were masked with RepeatMasker (http://www.repeatmasker.org/). Alignment of the resulting DNA sequences using Multipipmaker (http://pipmaker.bx.psu.edu/pipmaker/) revealed that the sequence conservation was maximal within a single short region (~300 bp) located upstream of the predicted transcription start site (http://genomatix.gsf.de/cgi-bin/dialign/dialign.pl). This region, with 37 nt from exon 1, was amplified by PCR from mouse tail genomic DNA (Supplementary Table S1). The PCR product was cloned in the pGL3-basic vector (Promega), placing the luc+ gene under the control of the SELENOT promoter (pGL3-SELENOT-306 vector). Two shorter SELENOT promoter fragments of 159 (pGL3-SELENOT-159) and 64 bp (pGL3-SELENOT-64) were amplified by PCR and cloned into the pGL3-Basic vector. Introduction of point mutations in the NRF-1 consensus sites was performed with the QuikChange II XL Site directed Mutagenesis kit (Agilent Technologies, Les Ulis, France) according to the instructions of the manufacturer. All constructs were verified by DNA sequencing (Beckman CEQ 8000/DNA Sequencer System, Beckman Coulter, Villepinte, France). Three putative NRF-1 binding sites were point-mutated on both sides of the palindromic binding site using appropriate primers (Supplementary Table S1).

Quantitative Real-Time PCR

Total RNA was extracted from PC12 cells using the TRI Reagent (Sigma-Aldrich) according to the manufacturer's protocol. Contaminating genomic DNA was removed by DNase I treatment, and 1 μg of total RNA was reverse-transcribed using the ImPromII™ Reverse-Transcription system (Promega). Real-time PCR was performed on the resulting cDNA using the Power SYBR Green® Master Mix (Life Technologies SAS, Division Applied Biosystems, Villebon-sur-Yvette, France) in the presence of 300 nM specific primers. Reactions were carried out using the ABI prism 7900HT Real-Time PCR System (Life Technologies SAS). All the results have been normalized using the Gapdh gene used as a reference. Data analysis was carried out using the 2(−Delta Delta C(T)) method ($2^{-\Delta(\Delta Ct)}$) and the results were presented as mean ± standard error of the mean (SEM) of at least three independent experiments, performed in triplicates. Primers used in this study are described in Supplementary Table S1.

Luciferase Assays

PC12 cells, grown in culture flasks until 80% confluency, were transiently co-transfected using the Amaxa Nucleofactor system (Lonza) with the SELENOT/firefly luciferase reporter constructs (pGL3-SELENOT plasmids) and the renilla luciferase control reporter. After cell lysis, luciferase activity was measured using the Dual-Luciferase Reporter Assay System (Promega) according to the manufacturer's instructions. Luminiscence was measured with a FlexstationIII^{96} fluorescence plate reader system (Molecular Devices, Saint-Grégoire, France). Results were obtained from at least three independent experiments performed in duplicate.

Chromatin Immunoprecipitation

PC12 cells, in basal conditions or after a treatment with PACAP (100 nM) for 6 h, were fixed 10 min at room temperature by 1% formaldehyde solution to crosslink DNA and proteins. After addition of glycine (0.25 M final concentration) to quench the crosslinking reaction and washing, the cells were resuspended in Tris-EDTA buffer containing protease inhibitors and 1% sodium dodecyl sulfate (SDS). Chromatin samples were sheared for 8 cycles of 30 s ON/30 s OFF with the Bioruptor® Pico apparatus (Diagenode, Paris, France) to obtain DNA fragments with an average size of 500 bp. ChIP experiments were performed using a previously described procedure [76] with a rabbit polyclonal anti-NRF-1 antibody ChIP Grade (Abcam) or the non-specific control rabbit polyclonal anti-furin antibody (Santa-Cruz Biotechnology, Heidelberg, Germany).

Immunohistochemistry

Immunocytochemistry was carried out on PC12 cells cultured in 12-well plates for 24 h and then treated with PACAP for 2 h. Cells were fixed in 4% paraformaldehyde for 20 min. A saturation step (1 h at room temperature) was performed with 1% normal goat serum diluted in a PBS solution containing 1% BSA and 0.3% Triton X-100, prior to overnight incubation with the mouse monoclonal NRF-1 primary antibody (1:2000) at 4 °C. An Alexa-conjugated goat anti-mouse (1:100) antibody (Invitrogen) was used as secondary antibodies. Nuclei were labeled with DAPI. Cells were examined with a Leica SP2 upright confocal laser scanning microscope (DMRAX-UV) equipped with the Acousto-Optico Beam Splitter system (Leica, Nanterre, France) on the Cell Imaging Platform of Normandy (PRIMACEN, Rouen).

Western Blot

PC12 cells were homogenized in lysis buffer (Cell Signaling Technology), supplemented by 20 mM NaF, 2 mM Na_3VO_4,

and protease inhibitors from Pierce (Thermo Fisher Scientific). Proteins were quantified using the Bradford method (Bio-Rad, Marnes-la-Coquette, France). Fifty micrograms was separated on SDS-PAGE gels (12%), and transferred onto a PVDF membrane (Thermo Fisher Scientific). Membranes were blocked for 1 h with a solution containing 5% milk in PBS, and incubated overnight at 4 °C with primary antibodies (1:1000 for p-AMPKα and AMPKα; 1:500 for SELENOT; 1:5000 for GAPDH and α-Tubulin; 1:1000 for PGC-1α; and 1:1000 for NRF-1) in 5% milk in PBS. Incubation with secondary antibodies (diluted 1:5000) was performed for 1 h at room temperature in the same solution. The antigen-antibody complexes were visualized by a chemiluminescence ECL western blotting analysis system, the Clarity Western ECL Substrate (Bio-Rad). Densitometric analysis was then performed using the Bio-Rad ChemiDoc illumination system with Image Lab software (Bio-Rad).

Co-immunoprecipitation

PC12 cells were homogenized at 4 °C with lysis buffer containing 50 mM Tris-HCl pH 7.5, 150 mM NaCl, 1% nonidet P40, 0.5% sodium deoxycholate supplemented with a protease inhibitor cocktail (Pierce, Thermo Fisher Scientific). Ten minutes later, the lysates were cleared by centrifugation at 14,000×*g* for 10 min at 4 °C and protein quantitated by the Bradford method. Co-immunoprecipitation was performed by incubating 2 mg of proteins at 4 °C overnight with 5 µg of a specific antibody and 25 µl of PureProteome Protein A/G magnetic beads (Millipore, Molsheim, France). Beads were washed three times with PBS-Tween buffer and denatured with 1× Laemmli buffer at 95 °C for 5 min. Samples were analyzed by SDS-PAGE and western blotting.

Mitochondrial DNA Quantification

PC12 cells were treated or not with PACAP for 72 h. Total DNA was extracted using the DNeasy blood & Tissue Kit (Qiagen, Courtaboeuf, France), according to the manufacturer's instructions. qPCR was performed as described above. The mtDNA content was measured by calculating the ratio of mitochondrial D-Loop region and Cyt b gene to the nuclear Pklr gene (Supplementary Table 1).

Flow Cytometry

PC12 cells were grown to 80–90% confluence on collagen I-coated plates in the absence or presence of PACAP-38 (100 nM) for 72 h, before staining with 50 nM MTG (MitoTrackerGreen; Life Technologies SAS), for 30 min in the dark at 37 °C. Cells were then washed in PBS, trypsinized, collected by centrifugation at 200×*g* for 5 min, and analyzed with a FACSCanto (BD Bioscience, Le Pont de Claix, France). Data were obtained from 2.10^4 cells for each sample and analyzed using the FlowJo software (Three Star, Ashland, OR, USA).

Statistical Analysis

All data were obtained from at least three independent experiments and expressed as means ± SEM or as mean ± standard deviation (SD). Statistical significance was assessed through nonparametric tests (Mann-Whitney *U* test, Wilcoxon test, one-way ANOVA), or using a two-way ANOVA. A probability level of P value < 0.05 was considered statistically significant.

Author Contributions I.L. and Y.A. designed the experiments. H.A., D.C, A.H., A-M.F-B., C.B., H.P., D-L.M. and A.S. performed the experiments; J.L. and O.B. helped to analyze the data, I.L. and Y.A. wrote the manuscript.

Funding This work was supported by Inserm (U1239), the Conseil Régional de Normandie, the University of Rouen Normandie and the European Union. Europe is involved in Normandie with European Regional Development Fund (ERDF).

Compliance with Ethical Standards

Competing Interests The authors declare they have no competing interest.

References

1. Francis NJ, Landis SC (1999) Cellular and molecular determinants of sympathetic neuron development. Annu Rev Neurosci 22:541–566. https://doi.org/10.1146/annurev.neuro.22.1.541
2. Anderson DJ (1993) Molecular control of cell fate in the neural crest: the sympathoadrenal lineage. Annu Rev Neurosci 16:129–158. https://doi.org/10.1146/annurev.ne.16.030193.001021
3. Huber K (2006) The sympathoadrenal cell lineage: specification, diversification, and new perspectives. Dev Biol 298:335–343. https://doi.org/10.1016/j.ydbio.2006.07.010
4. Emery AC, Eiden MV, Eiden LE (2014) Separate cyclic AMP sensors for neuritogenesis, growth arrest, and survival of neuroendocrine cells. J Biol Chem 289:10126–10139. https://doi.org/10.1074/jbc.M113.529321
5. Ravni A, Bourgault S, Lebon A, Chan P, Galas L, Fournier A, Vaudry H, Gonzalez B et al (2006) The neurotrophic effects of PACAP in PC12 cells: control by multiple transduction pathways. J Neurochem 98:321–329. https://doi.org/10.1111/j.1471-4159.2006.03884.x
6. Grumolato L, Louiset E, Alexandre D, Ait-Ali D, Turquier V, Fournier A, Fasolo A, Vaudry H et al (2003) PACAP and NGF regulate common and distinct traits of the sympathoadrenal lineage: effects on electrical properties, gene markers and transcription factors in differentiating PC12 cells. Eur J Neurosci 17:71–82
7. Ghzili H, Grumolato L, Thouennon E, Vaudry H, Anouar Y (2006) Possible implication of the transcriptional regulator Id3 in PACAP-induced pro-survival signaling during PC12 cell differentiation. Regul Pept 137:89–94. https://doi.org/10.1016/j.regpep.2006.06.015

8. Hamelink C, Tjurmina O, Damadzic R, Young WS, Weihe E, Lee HW, Eiden LE (2002) Pituitary adenylate cyclase-activating polypeptide is a sympathoadrenal neurotransmitter involved in catecholamine regulation and glucohomeostasis. Proc Natl Acad Sci U S A 99:461–466. https://doi.org/10.1073/pnas.012608999
9. Deutsch PJ, Sun Y (1992) The 38-amino acid form of pituitary adenylate cyclase-activating polypeptide stimulates dual signaling cascades in PC12 cells and promotes neurite outgrowth. J Biol Chem 267:5108–5113
10. Greene LA, Tischler AS (1976) Establishment of a noradrenergic clonal line of rat adrenal pheochromocytoma cells which respond to nerve growth factor. Proc Natl Acad Sci U S A 73:2424–2428
11. Kim T, Tao-Cheng JH, Eiden LE, Loh YP (2001) Chromogranin A, an "on/off" switch controlling dense-core secretory granule biogenesis. Cell 106:499–509
12. Montero-Hadjadje M, Vaingankar S, Elias S, Tostivint H, Mahata SK, Anouar Y (2008) Chromogranins A and B and secretogranin II: evolutionary and functional aspects. Acta Physiol (Oxf) 192:309–324. https://doi.org/10.1111/j.1748-1716.2007.01806.x
13. Grumolato L, Ghzili H, Montero-Hadjadje M, Gasman S, Lesage J, Tanguy Y, Galas L, Ait-Ali D et al (2008) Selenoprotein T is a PACAP-regulated gene involved in intracellular Ca2+ mobilization and neuroendocrine secretion. FASEB J 22:1756–1768. https://doi.org/10.1096/fj.06-075820
14. Hamieh A, Cartier D, Abid H, Calas A, Burel C, Bucharles C, Jehan C, Grumolato L et al (2017) Selenoprotein T is a novel OST subunit that regulates UPR signaling and hormone secretion. EMBO Rep 18:1935–1946. https://doi.org/10.15252/embr.201643504
15. Boukhzar L, Hamieh A, Cartier D, Tanguy Y, Alsharif I, Castex M, Arabo A, El Hajji S et al (2016) Selenoprotein T exerts an essential oxidoreductase activity that protects dopaminergic neurons in mouse models of Parkinson's disease. Antioxid Redox Signal 24:557–574. https://doi.org/10.1089/ars.2015.6478
16. Castex MT, Arabo A, Benard M, Roy V, Le Joncour V, Prevost G, Bonnet JJ, Anouar Y et al (2016) Selenoprotein T deficiency leads to neurodevelopmental abnormalities and hyperactive behavior in mice. Mol Neurobiol 53:5818–5832. https://doi.org/10.1007/s12035-015-9505-7
17. Tanguy Y, Falluel-Morel A, Arthaud S, Boukhzar L, Manecka DL, Chagraoui A, Prevost G, Elias S et al (2011) The PACAP-regulated gene selenoprotein T is highly induced in nervous, endocrine, and metabolic tissues during ontogenetic and regenerative processes. Endocrinology 152:4322–4335. https://doi.org/10.1210/en.2011-1246
18. Anouar Y, Lihrmann I, Falluel-Morel A, Boukhzar L (2018) Selenoprotein T is a key player in ER proteostasis, endocrine homeostasis and neuroprotection. Free Radic Biol Med. https://doi.org/10.1016/j.freeradbiomed.2018.05.076
19. Prevost G, Arabo A, Jian L, Quelennec E, Cartier D, Hassan S, Falluel-Morel A, Tanguy Y et al (2013) The PACAP-regulated gene selenoprotein T is abundantly expressed in mouse and human beta-cells and its targeted inactivation impairs glucose tolerance. Endocrinology 154:3796–3806. https://doi.org/10.1210/en.2013-1167
20. Rabinovitch RC, Samborska B, Faubert B, Ma EH, Gravel SP, Andrzejewski S, Raissi TC, Pause A et al (2017) AMPK maintains cellular metabolic homeostasis through regulation of mitochondrial reactive oxygen species. Cell Rep 21:1–9. https://doi.org/10.1016/j.celrep.2017.09.026
21. Botia B, Seyer D, Ravni A, Benard M, Falluel-Morel A, Cosette P, Jouenne T, Fournier A et al (2008) Peroxiredoxin 2 is involved in the neuroprotective effects of PACAP in cultured cerebellar granule neurons. J Mol Neurosci 36:61–72. https://doi.org/10.1007/s12031-008-9075-5
22. Grumolato L, Elkahloun AG, Ghzili H, Alexandre D, Coulouarn C, Yon L, Salier JP, Eiden LE et al (2003) Microarray and suppression subtractive hybridization analyses of gene expression in pheochromocytoma cells reveal pleiotropic effects of pituitary adenylate cyclase-activating polypeptide on cell proliferation, survival, and adhesion. Endocrinology 144:2368–2379. https://doi.org/10.1210/en.2002-0106
23. Miyamoto K, Tsumuraya T, Ohtaki H, Dohi K, Satoh K, Xu Z, Tanaka S, Murai N et al (2014) PACAP38 suppresses cortical damage in mice with traumatic brain injury by enhancing antioxidant activity. J Mol Neurosci 54:370–379. https://doi.org/10.1007/s12031-014-0309-4
24. Ohtaki H, Satoh A, Nakamachi T, Yofu S, Dohi K, Mori H, Ohara K, Miyamoto K et al (2010) Regulation of oxidative stress by pituitary adenylate cyclase-activating polypeptide (PACAP) mediated by PACAP receptor. J Mol Neurosci 42:397–403. https://doi.org/10.1007/s12031-010-9350-0
25. Satoh J, Kawana N, Yamamoto Y (2013) Pathway analysis of ChIP-Seq-based NRF1 target genes suggests a logical hypothesis of their involvement in the pathogenesis of neurodegenerative diseases. Gene Regul Syst Bio 7:139–152. https://doi.org/10.4137/GRSB.S13204
26. Scarpulla RC, Vega RB, Kelly DP (2012) Transcriptional integration of mitochondrial biogenesis. Trends Endocrinol Metab 23:459–466. https://doi.org/10.1016/j.tem.2012.06.006
27. Virbasius CA, Virbasius JV, Scarpulla RC (1993) NRF-1, an activator involved in nuclear-mitochondrial interactions, utilizes a new DNA-binding domain conserved in a family of developmental regulators. Genes Dev 7:2431–2445
28. Wu Z, Puigserver P, Andersson U, Zhang C, Adelmant G, Mootha V, Troy A, Cinti S et al (1999) Mechanisms controlling mitochondrial biogenesis and respiration through the thermogenic coactivator PGC-1. Cell 98:115–124. https://doi.org/10.1016/S0092-8674(00)80611-X
29. Knutti D, Kralli A (2001) PGC-1, a versatile coactivator. Trends Endocrinol Metab 12:360–365
30. St-Pierre J, Drori S, Uldry M, Silvaggi JM, Rhee J, Jager S, Handschin C, Zheng K et al (2006) Suppression of reactive oxygen species and neurodegeneration by the PGC-1 transcriptional coactivators. Cell 127:397–408. https://doi.org/10.1016/j.cell.2006.09.024
31. Wright DC, Han DH, Garcia-Roves PM, Geiger PC, Jones TE, Holloszy JO (2007) Exercise-induced mitochondrial biogenesis begins before the increase in muscle PGC-1alpha expression. J Biol Chem 282:194–199. https://doi.org/10.1074/jbc.M606116200
32. Fernandez-Marcos PJ, Auwerx J (2011) Regulation of PGC-1alpha, a nodal regulator of mitochondrial biogenesis. Am J Clin Nutr 93:884S–8890S. https://doi.org/10.3945/ajcn.110.001917
33. Austin S, St-Pierre J (2012) PGC1alpha and mitochondrial metabolism—emerging concepts and relevance in ageing and neurodegenerative disorders. J Cell Sci 125:4963–4971. https://doi.org/10.1242/jcs.113662
34. Kahn BB, Alquier T, Carling D, Hardie DG (2005) AMP-activated protein kinase: ancient energy gauge provides clues to modern understanding of metabolism. Cell Metab 1:15–25. https://doi.org/10.1016/j.cmet.2004.12.003
35. Hardie DG (2011) AMP-activated protein kinase: an energy sensor that regulates all aspects of cell function. Genes Dev 25:1895–1908. https://doi.org/10.1101/gad.17420111
36. Hardie DG (2014) AMPK—sensing energy while talking to other signaling pathways. Cell Metab 20:939–952. https://doi.org/10.1016/j.cmet.2014.09.013
37. Bergeron R, Ren JM, Cadman KS, Moore IK, Perret P, Pypaert M, Young LH, Semenkovich CF et al (2001) Chronic activation of AMP kinase results in NRF-1 activation and mitochondrial biogenesis. Am J Physiol Endocrinol Metab 281:E1340–E1346
38. Hutchinson DS, Summers RJ, Bengtsson T (2008) Regulation of AMP-activated protein kinase activity by G-protein coupled

receptors: potential utility in treatment of diabetes and heart disease. Pharmacol Ther 119:291–310. https://doi.org/10.1016/j.pharmthera.2008.05.008
39. Gascon S, Murenu E, Masserdotti G, Ortega F, Russo GL, Petrik D, Deshpande A, Heinrich C et al (2016) Identification and successful negotiation of a metabolic checkpoint in direct neuronal reprogramming. Cell Stem Cell 18:396–409. https://doi.org/10.1016/j.stem.2015.12.003
40. Ravni A, Eiden LE, Vaudry H, Gonzalez BJ, Vaudry D (2006) Cycloheximide treatment to identify components of the transitional transcriptome in PACAP-induced PC12 cell differentiation. J Neurochem 98:1229–1241. https://doi.org/10.1111/j.1471-4159.2006.03962.x
41. Seaborn T, Ravni A, Au R, Chow BK, Fournier A, Wurtz O, Vaudry H, Eiden LE et al (2014) Induction of Serpinb1a by PACAP or NGF is required for PC12 cells survival after serum withdrawal. J Neurochem. https://doi.org/10.1111/jnc.12780
42. Manecka DL, Lelievre V, Anouar Y (2014) Inhibition of constitutive TNF production is associated with PACAP-mediated differentiation in PC12 cells. FEBS Lett 588:3008–3014. https://doi.org/10.1016/j.febslet.2014.06.009
43. Manecka DL, Mahmood SF, Grumolato L, Lihrmann I, Anouar Y (2013) Pituitary adenylate cyclase-activating polypeptide (PACAP) promotes both survival and neuritogenesis in PC12 cells through activation of nuclear factor kappaB (NF-kappaB) pathway: involvement of extracellular signal-regulated kinase (ERK), calcium, and c-REL. J Biol Chem 288:14936–14948. https://doi.org/10.1074/jbc.M112.434597
44. Kienlen Campard P, Crochemore C, Rene F, Monnier D, Koch B, Loeffler JP (1997) PACAP type I receptor activation promotes cerebellar neuron survival through the cAMP/PKA signaling pathway. DNA Cell Biol 16:323–333
45. Vaudry D, Falluel-Morel A, Bourgault S, Basille M, Burel D, Wurtz O, Fournier A, Chow BK et al (2009) Pituitary adenylate cyclase-activating polypeptide and its receptors: 20 years after the discovery. Pharmacol Rev 61:283–357. https://doi.org/10.1124/pr.109.001370
46. Scarpulla RC (2006) Nuclear control of respiratory gene expression in mammalian cells. J Cell Biochem 97:673–683. https://doi.org/10.1002/jcb.20743
47. Hardie DG (2011) Sensing of energy and nutrients by AMP-activated protein kinase. Am J Clin Nutr 93:891S–8896S. https://doi.org/10.3945/ajcn.110.001925
48. Vazquez-Manrique RP, Farina F, Cambon K, Dolores Sequedo M, Parker AJ, Millan JM, Weiss A, Deglon N et al (2016) AMPK activation protects from neuronal dysfunction and vulnerability across nematode, cellular and mouse models of Huntington's disease. Hum Mol Genet 25:1043–1058. https://doi.org/10.1093/hmg/ddv513
49. Williams T, Courchet J, Viollet B, Brenman JE, Polleux F (2011) AMP-activated protein kinase (AMPK) activity is not required for neuronal development but regulates axogenesis during metabolic stress. Proc Natl Acad Sci U S A 108:5849–5854. https://doi.org/10.1073/pnas.1013660108
50. Dulovic M, Jovanovic M, Xilouri M, Stefanis L, Harhaji-Trajkovic L, Kravic-Stevovic T, Paunovic V, Ardah MT et al (2014) The protective role of AMP-activated protein kinase in alpha-synuclein neurotoxicity in vitro. Neurobiol Dis 63:1–11. https://doi.org/10.1016/j.nbd.2013.11.002
51. Dasgupta B, Milbrandt J (2007) Resveratrol stimulates AMP kinase activity in neurons. Proc Natl Acad Sci U S A 104:7217–7222. https://doi.org/10.1073/pnas.0610068104
52. Dasgupta B, Milbrandt J (2009) AMP-activated protein kinase phosphorylates retinoblastoma protein to control mammalian brain development. Dev Cell 16:256–270. https://doi.org/10.1016/j.devcel.2009.01.005
53. Stetler RA, Leak RK, Yin W, Zhang L, Wang S, Gao Y, Chen J (2012) Mitochondrial biogenesis contributes to ischemic neuroprotection afforded by LPS pre-conditioning. J Neurochem 123(Suppl 2):125–137. https://doi.org/10.1111/j.1471-4159.2012.07951.x
54. Salminen A, Kaarniranta K, Haapasalo A, Soininen H, Hiltunen M (2011) AMP-activated protein kinase: a potential player in Alzheimer's disease. J Neurochem 118:460–474. https://doi.org/10.1111/j.1471-4159.2011.07331.x
55. Ma TC, Buescher JL, Oatis B, Funk JA, Nash AJ, Carrier RL, Hoyt KR (2007) Metformin therapy in a transgenic mouse model of Huntington's disease. Neurosci Lett 411:98–103. https://doi.org/10.1016/j.neulet.2006.10.039
56. Shaw MM, Gurr WK, McCrimmon RJ, Schorderet DF, Sherwin RS (2007) 5′AMP-activated protein kinase alpha deficiency enhances stress-induced apoptosis in BHK and PC12 cells. J Cell Mol Med 11:286–298. https://doi.org/10.1111/j.1582-4934.2007.00023.x
57. Scarpulla RC (2002) Transcriptional activators and coactivators in the nuclear control of mitochondrial function in mammalian cells. Gene 286:81–89
58. Cam H, Balciunaite E, Blais A, Spektor A, Scarpulla RC, Young R, Kluger Y, Dynlacht BD (2004) A common set of gene regulatory networks links metabolism and growth inhibition. Mol Cell 16:399–411. https://doi.org/10.1016/j.molcel.2004.09.037
59. Kobayashi M, Yamamoto M (2006) Nrf2-Keap1 regulation of cellular defense mechanisms against electrophiles and reactive oxygen species. Adv Enzym Regul 46:113–140. https://doi.org/10.1016/j.advenzreg.2006.01.007
60. Miyamoto N, Izumi H, Miyamoto R, Kondo H, Tawara A, Sasaguri Y, Kohno K (2011) Quercetin induces the expression of peroxiredoxins 3 and 5 via the Nrf2/NRF1 transcription pathway. Invest Ophthalmol Vis Sci 52:1055–1063. https://doi.org/10.1167/iovs.10-5777
61. Chang C, Wu G, Gao P, Yang L, Liu W, Zuo J (2014) Upregulated Parkin expression protects mitochondrial homeostasis in DJ-1 knockdown cells and cells overexpressing the DJ-1 L166P mutation. Mol Cell Biochem 387:187–195. https://doi.org/10.1007/s11010-013-1884-3
62. Huo L, Scarpulla RC (2001) Mitochondrial DNA instability and peri-implantation lethality associated with targeted disruption of nuclear respiratory factor 1 in mice. Mol Cell Biol 21:644–654. https://doi.org/10.1128/MCB.21.2.644-654.2001
63. Larsson NG, Wang J, Wilhelmsson H, Oldfors A, Rustin P, Lewandoski M, Barsh GS, Clayton DA (1998) Mitochondrial transcription factor A is necessary for mtDNA maintenance and embryogenesis in mice. Nat Genet 18:231–236. https://doi.org/10.1038/ng0398-231
64. Becker TS, Burgess SM, Amsterdam AH, Allende ML, Hopkins N (1998) Not really finished is crucial for development of the zebrafish outer retina and encodes a transcription factor highly homologous to human Nuclear Respiratory Factor-1 and avian Initiation Binding Repressor. Development 125:4369–4378
65. DeSimone SM, White K (1993) The *Drosophila* erect wing gene, which is important for both neuronal and muscle development, encodes a protein which is similar to the sea urchin P3A2 DNA binding protein. Mol Cell Biol 13:3641–3649
66. Chang WT, Chen HI, Chiou RJ, Chen CY, Huang AM (2005) A novel function of transcription factor alpha-Pal/NRF-1: increasing neurite outgrowth. Biochem Biophys Res Commun 334:199–206. https://doi.org/10.1016/j.bbrc.2005.06.079
67. Evans MJ, Scarpulla RC (1990) NRF-1: a trans-activator of nuclear-encoded respiratory genes in animal cells. Genes Dev 4:1023–1034
68. Hawley SA, Pan DA, Mustard KJ, Ross L, Bain J, Edelman AM, Frenguelli BG, Hardie DG (2005) Calmodulin-dependent protein kinase kinase-beta is an alternative upstream kinase for AMP-

activated protein kinase. Cell Metab 2:9–19. https://doi.org/10.1016/j.cmet.2005.05.009
69. Collins SP, Reoma JL, Gamm DM, Uhler MD (2000) LKB1, a novel serine/threonine protein kinase and potential tumour suppressor, is phosphorylated by cAMP-dependent protein kinase (PKA) and prenylated in vivo. Biochem J 345(Pt 3):673–680
70. Vaudry D, Gonzalez BJ, Basille M, Anouar Y, Fournier A, Vaudry H (1998) Pituitary adenylate cyclase-activating polypeptide stimulates both c-fos gene expression and cell survival in rat cerebellar granule neurons through activation of the protein kinase A pathway. Neuroscience 84:801–812
71. Onoue S, Endo K, Ohshima K, Yajima T, Kashimoto K (2002) The neuropeptide PACAP attenuates beta-amyloid (1-42)-induced toxicity in PC12 cells. Peptides 23:1471–1478
72. Frodin M, Peraldi P, Van Obberghen E (1994) Cyclic AMP activates the mitogen-activated protein kinase cascade in PC12 cells. J Biol Chem 269:6207–6214
73. Villalba M, Bockaert J, Journot L (1997) Pituitary adenylate cyclase-activating polypeptide (PACAP-38) protects cerebellar granule neurons from apoptosis by activating the mitogen-activated protein kinase (MAP kinase) pathway. J Neurosci 17:83–90
74. Emery AC, Eiden LE (2012) Signaling through the neuropeptide GPCR PAC(1) induces neuritogenesis via a single linear cAMP- and ERK-dependent pathway using a novel cAMP sensor. FASEB J 26:3199–3211. https://doi.org/10.1096/fj.11-203042
75. Grumolato L, Liu G, Mong P, Mudbhary R, Biswas R, Arroyave R, Vijayakumar S, Economides AN et al (2010) Canonical and non-canonical Wnts use a common mechanism to activate completely unrelated coreceptors. Genes Dev 24:2517–2530. https://doi.org/10.1101/gad.1957710
76. Spencer VA, Sun JM, Li L, Davie JR (2003) Chromatin immunoprecipitation: a tool for studying histone acetylation and transcription factor binding. Methods 31:67–75